Int J Cardiovasc Imaging (2013) 29:1409–1416
DOI 10.1007/s10554-013-0225-7

ORIGINAL PAPER

First in vivo head-to-head comparison of high-definition versus standard-definition stent imaging with 64-slice computed tomography

Tobias A. Fuchs · Julia Stehli · Michael Fiechter · Svetlana Dougoud · Bert-Ram Sah · Cathérine Gebhard · Sacha Bull · Oliver Gaemperli · Philipp A. Kaufmann

Received: 15 February 2013 / Accepted: 19 April 2013 / Published online: 1 May 2013

Abstract The aim of this study was to compare image quality characteristics from 64-slice high definition (HDCT) versus 64-slice standard definition CT (SDCT) for coronary stent imaging. In twenty-five stents of 14 patients, undergoing contrast-enhanced CCTA both on 64-slice SDCT (LightSpeedVCT, GE Healthcare) and HDCT (Discovery HD750, GE Healthcare), radiation dose, contrast, noise and stent characteristics were assessed. Two blinded observers graded stent image quality (score 1 = no, 2 = mild, 3 = moderate, and 4 = severe artefacts). All scans were reconstructed with increasing contributions of adaptive statistical iterative reconstruction (ASIR) blending (0, 20, 40, 60, 80 and 100 %). Image quality was significantly superior in HDCT versus SDCT (score 1.7 ± 0.5 vs. 2.7 ± 0.7; $p < 0.05$). Image noise was significantly higher in HDCT compared to SDCT irrespective of ASIR contributions ($p < 0.05$). Addition of 40 % ASIR or more reduced image noise significantly in both HDCT and SDCT. In HDCT in-stent luminal attenuation was significantly lower and mean measured in-stent luminal diameter was significantly larger (1.2 ± 0.4 mm vs. 0.8 ± 0.4 mm; $p < 0.05$) compared to SDCT. Radiation dose from HDCT was comparable to SDCT (1.8 ± 0.7 mSv vs. 1.7 ± 0.7 mSv; p = ns). Use of HDCT for coronary stent imaging reduces partial volume artefacts from stents yielding improved image quality versus SDCT at a comparable radiation dose.

Keywords Coronary computed tomography angiography · Stent imaging · High definition CT · Iterative reconstruction

Introduction

Coronary computed tomography angiography (CCTA) has become a well-established non-invasive tool for diagnosis of coronary artery disease (CAD). While yielding high accuracy compared to invasive coronary angiography for the detection of coronary artery stenosis [1, 2], CCTA for stent imaging is still affected by artefacts from coronary stents leading to artificial luminal narrowing, due to partial volume artefact from highly attenuated stent struts [3, 4].

Although the in-stent restenosis rate has been substantially reduced by introducing drug-eluting stents it has not been entirely eliminated [5]. Furthermore, there is an increasing population of stented patients who are evaluated for progression of CAD. Therefore, any refinements in low radiation dose CCTA [2, 6] which may offer improved assessment of stents would be welcome.

Recently a new generation of high definition CT (HDCT) scanner (Discovery CT 750 HD, GE Healthcare, Milwaukee) has been introduced with substantially improved in plane resolution (0.23 mm × 0.23 mm) complemented by a new adaptive statistical iterative reconstruction (ASIR, GE Healthcare) algorithm in order to compensate for the increased noise due to the higher resolution [7]. Preliminary in vivo results have suggested that HDCT may provide superior evaluation of coronary stents

Tobias A. Fuchs and Julia Stehli contributed equally to this work.

T. A. Fuchs · J. Stehli · M. Fiechter · S. Dougoud · B.-R. Sah · C. Gebhard · S. Bull · O. Gaemperli · P. A. Kaufmann (✉)
Department of Radiology, Cardiac Imaging, University Hospital Zurich, Ramistrasse 100, NUK C 42, 8091 Zurich, Switzerland
e-mail: pak@usz.ch

P. A. Kaufmann
Zurich Center for Integrative Human Physiology (ZIHP), University of Zurich, Zurich, Switzerland

compared with SDCT [8]. Recent in vivo results seem to confirm that HDCT may improve image quality for coronary stents with 2.75–3.5 mm diameter compared with conventional standard definition CT (SDCT) due to higher spatial resolution [9], but those results were obtained from two different patient populations, one examined on a HDCT and the other on SDCT. Furthermore, the HDCT scans were reconstructed with latest reconstruction algorithms such as ASIR, while SDCT images were not. Thus, from that study, with relatively high radiation dose due to retrospective triggering, no firm conclusion on stent image quality from HDCT can be drawn. A recent elegant study has compared prospectively triggered low dose SDCT and HDCT using invasive coronary angiography and intravascular ultrasound as gold standard but did not provide head-to-head comparison of the two scanners in the same patients [10].

Therefore, the purpose of the present study was to compare the performance of 64-slice HDCT to 64-slice SDCT for coronary stent imaging of the same patients by assessing image quality as well as quantitative parameters, such as stent geometry and in-stent contrast attenuation.

Materials and methods

Study population

The study protocol was approved by the ethics committee, and written informed consent was obtained from all patients. Fourteen patients, who were referred by clinical indication for the assessment of CAD and had undergone previous percutaneous coronary intervention (PCI) with stent implantation were prospectively enrolled in the study. The patients underwent prospectively triggered contrast-enhanced CCTA both on a 64-slice SDCT (LightSpeed VCT, GE Healthcare) and HDCT scanner (Discovery HD 750, GE Healthcare) on the same day. Exclusion criteria were known hypersensitivity to iodinated contrast agent, renal insufficiency (glomerular filtration rate < 60 ml/min), non-sinus rhythm.

CCTA acquisition and reconstruction

Prior to the examination metoprolol (up to 25 mg Beloc, AtraZeneca, London, UK) was injected intravenously if heart rate was higher than 65 beats per minute and 2.5 mg isosorbiddinitrate (Isoket, Schwarz Pharma, Monheim, Germany) was administered sublingually in order to obtain optimal image quality for CCTA. All patients underwent contrast-enhanced CCTA during inspiration breath hold with prospective ECG-triggering as previously reported [2, 11, 12] on a SDCT (LightSpeedVCT, GE Healthcare) and a HDCT (Discovery HD 750, GE Healthcare) scanner. Iodixanol (Visipaque 320, 320 mg/ml, GE Healthcare) was injected into an antecubital vein followed by 50 ml saline solution. Contrast media volume (40 -105 ml) and flow rate (3.5–5 ml/s) were adapted to body surface area (BSA) as previously validated [13].

Scanning parameters of SDCT and HDCT were as follows: Collimation of 64×0.625 mm, gantry rotation time of 0.35 s and field of view was 25 cm. Tube voltage (100–120 kV) and tube current (450–700 mA) were adapted to body mass index as previously described [14]. Scans of HDCT were acquired in high resolution mode with an in-plane spatial resolution of 0.23 mm $\times$ 0.23 mm as previously reported [7]. All scans of SDCT and HDCT were reconstructed using FBP (0 % ASIR) and increasing ASIR blending factors, i.e. 20, 40, 60, 80 and 100 %. The iterative reconstruction algorithm ASIR has been described in detail previously [15–17]. In brief, ASIR reconstructs pictures by comparing measured projection with a synthesized projection using both statistical fluctuation calculations and system optics.

Radiation dose

Effective radiation dose from CCTA was calculated as the product of dose-length product (DLP) times a conversion coefficient for chest ($k = 0.014$ mSv mGy^{-1} cm^{-1}) [18].

Stent visualization and image quality

All images were transferred to an external workstation (AW 4.6, GE Healthcare) for analysis. Qualitative stent analysis was performed by two independent, experienced coronary CCTA readers, blinded for scanner type, clinical history, indication, and stent characteristics. Axial slices as well as curved multiplanar reformations were analysed using a window width of 1200 HU and window level of 240 HU. Image quality was evaluated on a 4-point Likert score for each stent as previously reported (adapted) [19]. Score 1: no artefacts in the surrounding of the stent; score 2: minor artefacts; score 3: major artefacts partially obscuring the stent surrounding; score 4: severe artefacts affecting diagnostic information. Reasons for impaired image quality (stents scored 2–4) were classified as partial volume artefacts, motion artefacts, or calcifications.

Attenuation measurements

Image signal and noise were determined by placing a circled region of interest (ROI) with 20 mm diameter in the aortic root and defined as the mean attenuation value and its standard deviation. Furthermore attenuation was measured within the stent lumen as well as 5 mm proximal and 5 mm distal to the stent. ROIs were drawn as large as possible, carefully avoiding calcifications, stenosis, stents struts or streak artefacts. To ensure that the same location was measured in all reconstructions an automated tool was used (Compare Viewer, GE Healthcare, Milwaukee).

Stent geometry

In order to standardize the analysis luminal diameter as well as stent length were measured in curved multiplanar reconstructions using a zoomed field of view with a fixed window level at 240 HU and window width of 1200 HU. Several measurements were performed (depending on the stent length) to assess the in-stent luminal diameter by using electronic callipers, and all measurements were averaged for each stent. The stent length was measured at both vessel borders and values were averaged (Fig. 1).

Statistical analysis

Quantitative variables were expressed as mean ± standard deviation (SD) and categorical variables as frequencies or percentages. The statistical software package SPSS 20.0 (SPSS, Chicago, IL) was used for analysis. For image quality inter-observer agreements were expressed as Cohen κ statistics and interpreted as previously reported [20]: $\kappa \leq 0.2$: poor agreement, $0.2 < \kappa \leq 0.4$: fair agreement, $0.4 < \kappa \leq 0.6$: moderate agreement; $0.6 < \kappa \leq 0.8$: good agreement; $0.8 < \kappa \leq 1.0$: excellent agreement. Wilcoxon signed rank test was used to analyse subjective image quality. The data were tested for normal distribution by Shapiro–Wilk test. Comparison of variables with no normal distribution were performed with Mann-Withney U, comparisons of continuous variables with normal distributions between groups were performed with tow-sided Student *t* test and analysis of variance. P values of less than 0.05 were considered statistically significant.

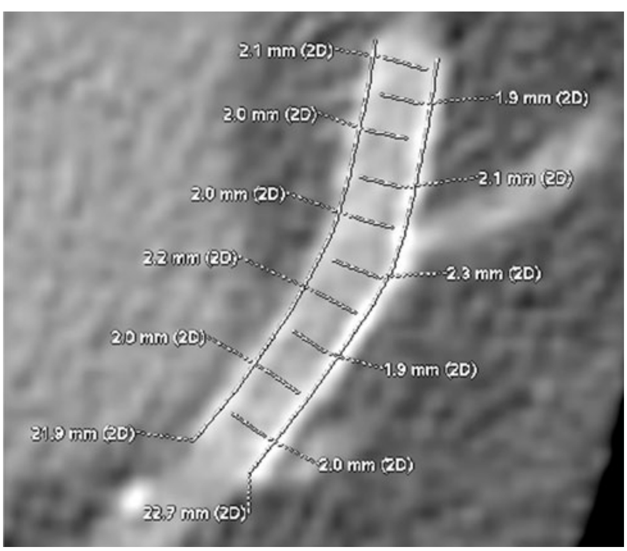

Fig. 1 Stent in LAD scanned with 64-slice HDCT (reconstructed with 0 % ASIR) illustrating the method of stent diameter and stent length measurement in curved multiplanar reconstruction

Results

Study population

Fourteen patients with twenty-five stents (1–5 stents per patient, mean 1.8 ± 1.3) were scanned 3.7 ± 3.4 years after stent implantation with 64-slice HDCT and SDCT at a mean age of 63.0 ± 9.8 years and mean body mass index of 29.8 ± 4.3 kg/m^2 (range 24.9–37.8 kg/m^2). After intravenous administration of 10 ± 9 mg beta blocker, the average heart rate during HDCT and SDCT scan was 55.9 ± 5.7 and 55.2 ± 7.7 beats per minute (p = ns), with an mean heart rate variability of 2.4 ± 3.3 and 3.8 ± 8.0 beats per minute (p = ns). The mean interval between the two scans was 31 ± 34 min. The patient baseline characteristics are presented in Table 1.

Stent characteristics and location

Twenty-five stents were analysed in the left anterior descending artery (LAD; $n = 15$), in the left circumflex

Table 1 Patient characteristics ($n = 14$)

Characteristics	Value
Age (mean ± SD, years)	63.0 ± 9.8
BMI (mean ± SD, kg/m^2)	29.8 ± 4.3
HR during HDCT	56 ± 6
HR during SDCT	55 ± 8
Stent localization	
LAD	15 (60 %)
LCX	2 (8 %)
RCA	3 (12 %)
PDA	3 (12 %)
Diagonal branch	1 (4 %)
Intermediate branch	1 (4 %)
Cardiovascular risk factors	
Hypertension	9 (64.2 %)
Dyslipidemia	9 (64.2 %)
Smoking	9 (64.2 %)
Diabetes	6 (42.9 %)
Positive family history	0 (0.0 %)

SD standard deviation; *BMI* body mass index; *HR* heart rate; *HDCT* high definition computed tomography; *SDCT* standard definition computed tomography; *LAD* left anterior descending; *LCX* left circumflex artery; *RCA* right coronary artery; *PDA* posterior descending artery

artery (LCX; $n = 2$), in the right coronary artery (RCA; $n = 3$), in the posterior descending artery (PDA; $n = 3$) and in side branches ($n = 2$). There were 10 different types of stents implanted in the patients, i.e. Cypher (Cordis, Miami, FL, USA; $n = 8$), Resolute Integrity (Medtronic Vascular, Santa Rosa, CA; $n = 4$), Endeavor (Medtronic, Minn; $n = 3$), Biomatrix (Biosensors Interventional Technologies Pte Ltd., Singapore; $n = 3$), Presillion (Cordis Corp., Miami, FL; $n = 1$), PRO-Kinetic (Biotronic, Switzerland; $n = 1$), Driver (Medtronic, Natick, MA, USA; $n = 2$), Xience prime (Abbott Vascular, Santa Clara, CA, USA; $n = 1$), Nobori (Terumo Corporation, Tokyo, Japan; $n = 1$) and Taxus (Boston Scientific, Boston, MA, USA; $n = 1$).

Radiation dose

The mean radiation dose of CCTA was 1.8 ± 0.7 mSv from HDCT and 1.7 ± 0.7 mSv from SDCT (p = ns).

Image quality

All 25 stents could be visualized with both HDCT and SDCT. In HDCT versus SDCT stents without artefacts (score 1) were found in 32 versus 0 % ($n = 8$ vs. 0), minor artefacts (score 2) were found in 64 versus 44 % ($n = 16$ vs. 11), moderate artefacts (score 3) were found in 4 versus 40 % ($n = 1$ vs. 10) and severe artefacts (score 4) were found in 0 versus 16 % ($n = 0$ vs. 4; Fig. 2). Reasons for impaired image quality in HDCT and SDCT were partial volume artefacts in 32 and 56 % ($n = 8$ and 14), motion artefacts in 4 and 12 % ($n = 1$ and 3) and calcifications in 32 and 32 % ($n = 8$ and 8). The use of HDCT increased the number of stents with no or minor artefacts significantly from 44 to 96 % ($p < 0.05$). Mean image quality score was significantly superior in HDCT versus SDCT for 0, 60, and 100 % ASIR (Table 2; $p < 0.05$), revealing highest image quality by HDCT with 60 % ASIR. Inter-observer analysis showed good agreement (κ = 0.8).

Attenuation measurements

There was no significant difference in mean signal of the ascending aorta in HDCT and SDCT (434.6 ± 85.7 and 438.3 ± 86.1 p = ns). Addition of different ASIR contributions had no impact on the latter values in both scanners (p = ns). Image noise was significantly higher in HDCT compared with SDCT in all ASIR reconstructions ($p < 0.05$). Compared to FBP reconstruction (0 % ASIR), in both HDCT and SDCT, image noise was significantly reduced using 40 % of ASIR or more, up to a noise reduction of 48 % in HDCT and 41 % in SDCT (Fig. 3).

In-stent luminal attenuation was significantly lower in HDCT compared to SDCT in all ASIR reconstructions ($p < 0.05$), whereas no significant difference was measured proximal or distal to the stents (Table 3).

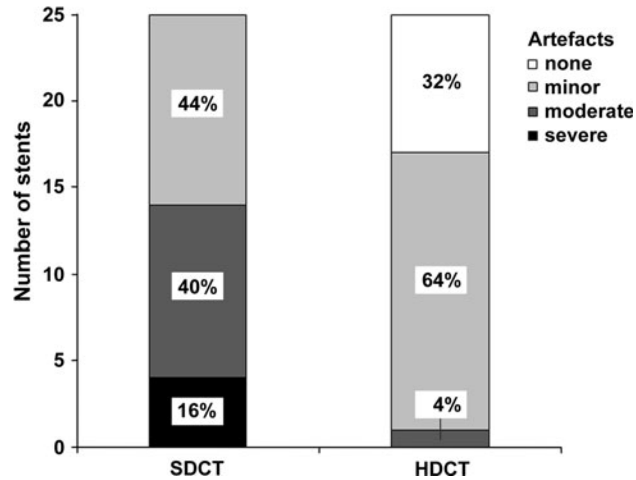

Fig. 2 Image quality score of stents scanned with SDCT and HDCT (0 % ASIR)

Table 2 Comparison of image quality scores in SDCT and HDCT images

Scanner	0 % ASIR	60 % ASIR	100 % ASIR
SDCT	2.7 ± 0.7	2.9 ± 0.6	$3.4 \pm 0.8^{+}$
HDCT	1.7 ± 0.5*	1.5 ± 0.6*	$2.2 \pm 0.8^{*,+}$

Image quality scores in standard definition computed tomography (SDCT) and high definition computed tomography (HDCT)

* $p < 0.05$ versus SDCT, $^{+}$ p <0.05 versus 0 % ASIR

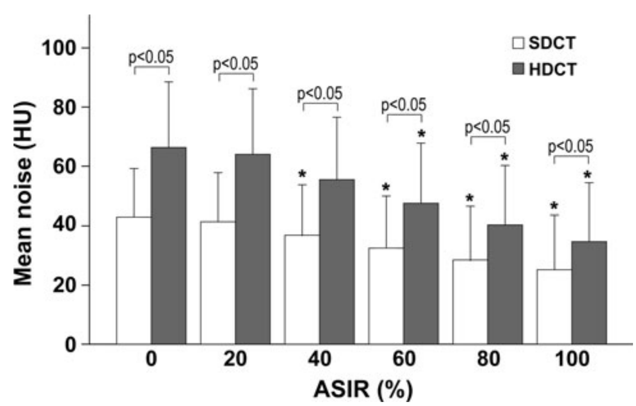

Fig. 3 While there was no significant difference in mean signal of the ascending aorta in SDCT and HDCT, noise was significantly higher in HDCT compared to SDCT ($p < 0.05$). In addition compared to 0 % ASIR noise was significantly reduced by increasing contributions of ASIR (* $p < 0.05$)

Stent geometry

The mean measured in-stent luminal diameter was significantly larger in HDCT than in SDCT (1.2 ± 0.4 mm vs.

Table 3 Comparison of CT attenuation measurements on SDCT and HDCT images

Location of measurement	Scanner	0 % ASIR	20 % ASIR	40 % ASIR	60 % ASIR	80 % ASIR	100 % ASIR
In-stent lumen	SDCT	598.3 ± 124.2	586.2 ± 126.9	588.8 ± 127.4	591.5 ± 128.1	594.4 ± 129.2	592.0 ± 131.2
	HDCT	474.1 ± 108.1	450.0 ± 110.5	456.0 ± 124.6	453.1 ± 112.2	456.1 ± 110.2	447.7 ± 116.3
		$p < 0.05$	$p < 0.05$	$p < 0.05$	$p < 0.05$	$p < 0.05$	$p < 0.05$
Proximal to stent*	SDCT	396.0 ± 90.0*	387.1 ± 89.7*	383.9 ± 90.2*	380.7 ± 90.8*	377.6 ± 91.6*	374.3 ± 92.6*
	HDCT	396.1 ± 88.9*	403.4 ± 87.4*	395.5 ± 88*	390.9 ± 87.1*	386.2 ± 83.8*	381.2 ± 83.8*
		p = ns	p = ns	p = ns	p = ns	p = ns	p = ns
Distal to stent*	SDCT	351.8 ± 88.8*	360.4 ± 93.3*	351.1 ± 94.6*	342.0 ± 96.4*	332.8 ± 98.4*	323.6 ± 100.8
	HDCT	342.4 ± 91.6*	349.8 ± 90.7*	345.0 ± 90.8*	340.0 ± 91.3*	335.2 ± 92.2*	325.4 ± 93.8*
		p = ns	p = ns	p = ns	p = ns	p = ns	p = ns

Data are attenuation values in Hounsfield units given as mean ± SD

SDCT standard definition computed tomography, *HDCT* high definition computed tomography

* $p < 0.05$ for each values versus in-stent

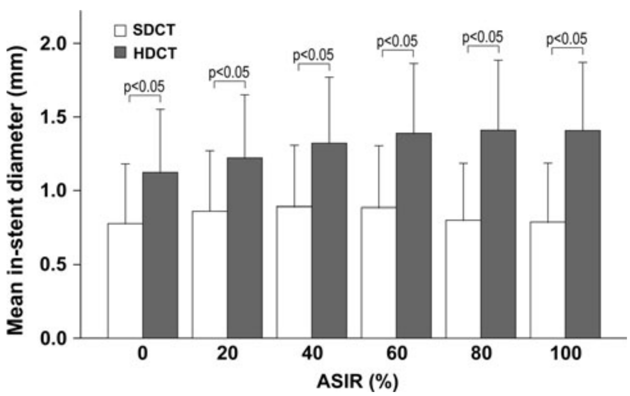

Fig. 4 The mean measured in-stent luminal diameter was significantly higher in HDCT than in SDCT ($p < 0.05$) while no significant difference in stent length was measured

0.8 ± 0.4 mm, 0 %ASIR; $p < 0.05$), which also holds true for all ASIR reconstructions. Addition of increasing ASIR contributions had no impact on the in-stent luminal diameter in SDCT (0.8 ± 0.4 mm, 100 % ASIR), while it tended to increase in HDCT (1.4 ± 0.5 mm, 100 % ASIR) although the comparison to FBP fell short of statistical significance (Fig. 4).

There was no significant difference in mean measured stent length in HDCT and SDCT (23.4 ± 8.3 mm vs. 23.8 ± 8.3 mm, 0 %ASIR; p = ns), which remained unaffected by ASIR. Figure 5 demonstrates a representative stent scanned in HDCT and SDCT reconstructed with all ASIR contributions.

Discussion

This study reports on the first head-to-head comparison of the in vivo visualisation and quantitative assessment of coronary stents using a latest generation HDCT versus SDCT. The main finding is the fact that partial volume effects were significantly reduced by HDCT scanning. As a result, the proportion of stents imaged successfully with no or only minor artefacts increased substantially from 44 to 96 % of stents by HDCT, underlining that partial volume effects represent a major limitation of coronary stent imaging by SDCT.

Although the rate of restenosis has substantially decreased over the past years, it remains a non-negligible drawback of coronary stenting. Therefore, a reliable non-invasive diagnostic imaging tool for differentiation of in-stent restenosis from progression of CAD in non-stented segments remains highly desirable. CCTA has rapidly evolved over the past years into a widely used alternative of conventional invasive coronary angiography supported by a growing body of literature. However, visualization and therefore robust evaluation of stents by SDCT has been hampered so far by high attenuation of the stent material interacting with the luminal contrast material attenuation due to blooming and partial volume artefacts. The latter artificially increase the measured in-stent attenuation (increase in HU) and decrease the apparent stent lumen diameter therefore affecting the image interpretation. The HDCT was designed to allow an increase in spatial resolution (0.23 mm × 0.23 mm) by delivering more views per rotation and integrating a new detector. In our study the latter was paralleled by an increase in noise, which is in line with previous studies [16]. Therefore this technical refinement has been complemented by new reconstruction algorithms such as ASIR to compensate for the noise increase [21]. In our study in both, HDCT and SDCT scanning, image noise was significantly reduced using 40 % of ASIR or more, whereas this had no impact on the mean signal.

Although the HDCT provides a high spatial resolution in this study radiation dose was comparable to SDCT scans.

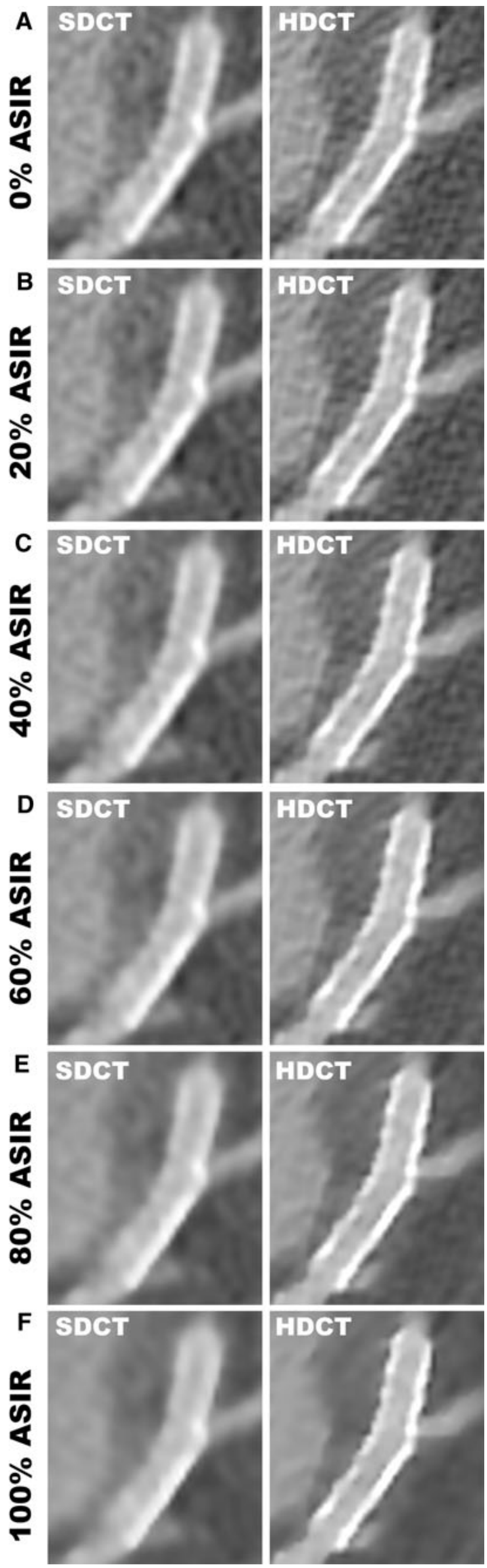

◀**Fig. 5** Curved multiplanar reconstruction of a stent scanned with 64-slice SDCT (*left column*) and HDCT (*right column*) reconstructed by 0 % ASIR (**a**), 20 % ASIR (**b**), 40 % ASIR (**c**), 60 % ASIR (**d**), 80 % ASIR (**e**) and 100 % ASIR (**f**)

As the potential carcinogenic risk of CCTA has been vividly and extensively discussed and put controversially into perspective of the potential benefits of the method [22], it is very important to note that despite using HDCT, the prospective ECG triggering protocol still allows low dose CCTA yielding a mean radiation dose (1.8 ± 0.7 mSv) comparable to or even lower than reported in other CCTA studies [12, 23–25].

In vitro stent imaging analyses have shown that artefacts from coronary stents leading to artificial luminal narrowing, due to partial volume artefact from highly attenuated stent struts vary depending on the stent material [26]. Most severe artefacts have been observed in tantalum or gold-coated stents. Therefore a large variety of different stents has been included in our study in order to represent a large variety of artefact severity.

Recent studies reported that in-stent lumen cannot be interpreted in up to 42 % of coronary stents [27, 28]. Nevertheless, recent guidelines on coronary revascularization include a recommendation for CCTA follow up in patients after unprotected left main stenting [29]. This is probably due—at least in past—to the fact that stent imaging by CCTA has improved due to advancements in CT technology, particularly after introduction of 64-slice CT. Introduction of HDCT is a further promising step to improve stent image visualization and interpretation. However, whether this may translate into higher accuracy of in-stent restenosis or stenosis severity of calcified lesions remains to be evaluated. Therefore, it may be perceived as limitation of the present study that diagnostic accuracy and in-stent luminal-diameter-measurement was not compared to invasive coronary angiography as a ground of truth reference standard. Furthermore, our analysis was not performed separately for each stent due to the limited stent number in each group. However, the fact that the results are consistent with 10 different stent types further strengthens our study.

In conclusion the use of HDCT for coronary stent imaging reduces partial volume artefacts from stents yielding improved image quality versus SDCT at a comparable radiation dose.

Acknowledgments The study was supported by grants from the Swiss National Science Foundation to PAK and MF. We also gratefully acknowledge the financial support of the Swiss Life Jubiläumsstiftung. Furthermore, we thank our technicians, Ennio Mueller and Gentian Cermjani for their excellent technical support.

Conflict of interest None declared.

Ethical Standard All procedures followed were in accordance with the ethical standards of the responsible committee on human experimentation (institutional and national) and with the Helsinki Declaration of 1975 as revised in 2008 (5). Informed consent was obtained from all patients for being included in the study.

References

1. Schroeder S, Achenbach S, Bengel F, Burgstahler C, Cademartiri F, de Feyter P, George R, Kaufmann P, Kopp AF, Knuuti J, Ropers D, Schuijf J, Tops LF, Bax JJ (2008) Cardiac computed tomography: indications, applications, limitations, and training requirements: report of a writing group deployed by the working group nuclear cardiology and cardiac CT of the European society of cardiology and the European council of nuclear cardiology. Eur Heart J 29(4):531–556
2. Herzog BA, Husmann L, Burkhard N, Gaemperli O, Valenta I, Tatsugami F, Wyss CA, Landmesser U, Kaufmann PA (2008) Accuracy of low-dose computed tomography coronary angiography using prospective electrocardiogram-triggering: first clinical experience. Eur Heart J 29(24):3037–3042
3. Kruger S, Mahnken AH, Sinha AM, Borghans A, Dedden K, Hoffmann R, Hanrath P (2003) Multislice spiral computed tomography for the detection of coronary stent restenosis and patency. Int J Cardiol 89(2–3):167–172
4. Maintz D, Juergens KU, Wichter T, Grude M, Heindel W, Fischbach R (2003) Imaging of coronary artery stents using multislice computed tomography: in vitro evaluation. Eur Radiol 13(4):830–835
5. Morice MC, Colombo A, Meier B, Serruys P, Tamburino C, Guagliumi G, Sousa E, Stoll HP (2006) Sirolimus- vs paclitaxel-eluting stents in de novo coronary artery lesions: the REALITY trial: a randomized controlled trial. JAMA 295(8):895–904
6. Husmann L, Valenta I, Gaemperli O, Adda O, Treyer V, Wyss CA, Veit-Haibach P, Tatsugami F, von Schulthess GK, Kaufmann PA (2008) Feasibility of low-dose coronary CT angiography: first experience with prospective ECG-gating. Eur Heart J 29(2):191–197
7. Kazakauskaite E, Husmann L, Stehli J, Fuchs T, Fiechter M, Klaeser B, Ghadri JR, Gebhard C, Gaemperli O, Kaufmann PA (2012) Image quality in low-dose coronary computed tomography angiography with a new high-definition CT scanner. Int J Cardiovasc Imaging 29:471–477
8. Min JK, Swaminathan RV, Vass M, Gallagher S, Weinsaft JW (2009) High-definition multidetector computed tomography for evaluation of coronary artery stents: comparison to standard-definition 64-detector row computed tomography. J Cardiovasc Comput Tomogr 3(4):246–251
9. Yang WJ, Zhang H, Xiao H, Li JY, Liu Y, Pan ZL, Chen KM (2012) High-definition computed tomography for coronary artery stents imaging compared with standard-definition 64-row multidectector computed tomography: an initial in vivo study. J Comput Assist Tomogr 36(3):295–300
10. Andreini D, Pontone G, Mushtaq S, Bartorelli AL, Bertella E, Trabattoni D, Montorsi P, Galli S, Foti C, Annoni A, Bovis F, Ballerini G, Agostoni P, Fiorentini C, Pepi M (2012) Coronary in-stent restenosis: assessment with CT coronary angiography. Radiology 265(2):410–417
11. Husmann L, Schepis T, Scheffel H, Gaemperli O, Leschka S, Valenta I, Koepfli P, Desbiolles L, Stolzmann P, Marincek B, Alkadhi H, Kaufmann PA (2008) Comparison of diagnostic accuracy of 64-slice computed tomography coronary angiography in patients with low, intermediate, and high cardiovascular risk. Acad Radiol 15(4):452–461
12. Buechel RR, Husmann L, Herzog BA, Pazhenkottil AP, Nkoulou R, Ghadri JR, Treyer V, von Schulthess P, Kaufmann PA (2011) Low-dose computed tomography coronary angiography with prospective electrocardiogram triggering: feasibility in a large population. J Am Coll Cardiol 57(3):332–336
13. Pazhenkottil AP, Husmann L, Buechel RR, Herzog BA, Nkoulou R, Burger IA, Vetterli A, Valenta I, Ghadri JR, von Schulthess P, Kaufmann PA (2010) Validation of a new contrast material protocol adapted to body surface area for optimized low-dose CT coronary angiography with prospective ECG-triggering. Int J Cardiovasc Imaging 26(5):591–597
14. Tatsugami F, Husmann L, Herzog BA, Burkhard N, Valenta I, Gaemperli O, Kaufmann PA (2009) Evaluation of a body mass index-adapted protocol for low-dose 64-MDCT coronary angiography with prospective ECG triggering. AJR Am J Roentgenol 192(3):635–638
15. Fuchs TA, Fiechter M, Gebhard C, Stehli J, Ghadri JR, Kazakauskaite E, Herzog BA, Husmann L, Gaemperli O, Kaufmann PA (2012) CT coronary angiography: impact of adapted statistical iterative reconstruction (ASIR) on coronary stenosis and plaque composition analysis. Int J Cardiovasc Imaging 29:719–724
16. Leipsic J, Labounty TM, Heilbron B, Min JK, Mancini GB, Lin FY, Taylor C, Dunning A, Earls JP (2010) Adaptive statistical iterative reconstruction: assessment of image noise and image quality in coronary CT angiography. AJR Am J Roentgenol 195(3):649–654
17. Gebhard C, Fiechter M, Fuchs TA, Ghadri JR, Herzog BA, Kuhn F, Stehli J, Muller E, Kazakauskaite E, Gaemperli O, Kaufmann PA (2012) Coronary artery calcium scoring: Influence of adaptive statistical iterative reconstruction using 64-MDCT. Int J Cardiol. doi:10.1016/j.ijcard.2012.08.003
18. Ghadri JR, Kuest SM, Goetti R, Fiechter M, Pazhenkottil AP, Nkoulou RN, Kuhn FP, Pietsch C, von Schulthess P, Gaemperli O, Templin C, Kaufmann PA (2012) Image quality and radiation dose comparison of prospectively triggered low-dose CCTA: 128-slice dual-source high-pitch spiral versus 64-slice single-source sequential acquisition. Int J Cardiovasc Imaging 28(5):1217–1225
19. Schepis T, Koepfli P, Leschka S, Desbiolles L, Husmann L, Gaemperli O, Eberli FR, Wildermuth S, Marincek B, Luscher TF, Alkadhi H, Kaufmann PA (2007) Coronary artery stent geometry and in-stent contrast attenuation with 64-slice computed tomography. Eur Radiol 17(6):1464–1473
20. Landis JR, Koch GG (1977) An application of hierarchical kappa-type statistics in the assessment of majority agreement among multiple observers. Biometrics 33(2):363–374
21. Gebhard C, Fiechter M, Fuchs TA, Stehli J, Muller E, Stahli BE, Gebhard CE, Ghadri JR, Klaeser B, Gaemperli O, Kaufmann PA (2013) Coronary artery stents: influence of adaptive statistical iterative reconstruction on image quality using 64-HDCT. Eur Heart J Cardiovasc Imaging. doi:10.1093/ehjci/jet013
22. Kaufmann PA, Knuuti J (2011) Ionizing radiation risks of cardiac imaging: estimates of the immeasurable. Eur Heart J 32(3):269–271
23. Herzog BA, Wyss CA, Husmann L, Gaemperli O, Valenta I, Treyer V, Landmesser U, Kaufmann PA (2009) First head-to-head comparison of effective radiation dose from low-dose 64-slice CT with prospective ECG-triggering versus invasive coronary angiography. Heart 95(20):1656–1661
24. Husmann L, Herzog BA, Gaemperli O, Tatsugami F, Burkhard N, Valenta I, Veit-Haibach P, Wyss CA, Landmesser U, Kaufmann PA (2009) Diagnostic accuracy of computed tomography coronary angiography and evaluation of stress-only single-photon emission computed tomography/computed tomography hybrid

imaging: comparison of prospective electrocardiogram-triggering versus retrospective gating. Eur Heart J 30(5):600–607
25. Dewey M, Zimmermann E, Deissenrieder F, Laule M, Dubel HP, Schlattmann P, Knebel F, Rutsch W, Hamm B (2009) Noninvasive coronary angiography by 320-row computed tomography with lower radiation exposure and maintained diagnostic accuracy: comparison of results with cardiac catheterization in a head-to-head pilot investigation. Circulation 120(10):867–875
26. Maintz D, Seifarth H, Raupach R, Flohr T, Rink M, Sommer T, Ozgun M, Heindel W, Fischbach R (2006) 64-slice multidetector coronary CT angiography: in vitro evaluation of 68 different stents. Eur Radiol 16(4):818–826
27. Manghat N, Van Lingen R, Hewson P, Syed F, Kakani N, Cox I, Roobottom C, Morgan-Hughes G (2008) Usefulness of 64-detector row computed tomography for evaluation of intracoronary stents in symptomatic patients with suspected in-stent restenosis. Am J Cardiol 101(11):1567–1573
28. Cademartiri F, Maffie E, Palumbo A, Martini C, Aldrovandi A, Ardissino D, Brambilla V, Coruzzi P, Mollet NR, Krestin GP, de Feyter PJ (2010) CT coronary angiography for the follow-up of coronary stent. Acta Biomed 81(2):87–93
29. Wijns W, Kolh P, Danchin N, Di Mario C, Falk V, Folliguet T, Garg S, Huber K, James S, Knuuti J, Lopez-Sendon J, Marco J, Menicanti L, Ostojic M, Piepoli MF, Pirlet C, Pomar JL, Reifart N, Ribichini FL, Schalij MJ, Sergeant P, Serruys PW, Silber S, Sousa Uva M, Taggart D (2010) Guidelines on myocardial revascularization. Eur Heart J 31(20):2501–2555